Factors influencing osteogenic differentiation of human aortic valve interstitial cells

Tingwen Zhou, MD,[a] Dong Han, MD,[b] Junwei Liu, MD,[a] Jiawei Shi, MD,[a] Peng Zhu, MD,[a] Yongjun Wang, MD,[a] and Nianguo Dong, MD[a]

ABSTRACT

Objective: Human aortic valve interstitial cells redifferentiate into an osteoblast-like phenotype, which is the key cellular mechanism of aortic valve calcification. Methyltransferase-like 3, the N6-methyladenosine methylation writer, has emerged as a new layer of epigenetic regulation for osteogenic differentiation of bone mesenchymal stem cells. The current study sought to determine whether methyltransferase-like 3 also plays a role in the osteogenic differentiation of human aortic valve interstitial cells.

Methods: Aortic valves from patients with aortic stenosis (n = 50) and normal controls (n = 50) were subjected to determination of methyltransferase-like 3 expression. Mineralized bone matrix formation was assessed by Alizarin Red staining. The interaction between methyltransferase-like 3 and twist-related protein 1 was confirmed via luciferase reporter and N6-methyladenosine methylated RNA immunoprecipitation quantitative reverse-transcription polymerase chain reaction.

Results: Methyltransferase-like 3 was highly expressed in human calcified aortic valves (1.61 ± 0.50) versus normal valves (3.07 ± 0.62; P < .0001). Osteogenic stimulation for 7 days resulted in a 2.15 ± 0.16-fold increase (P < .0001) in methyltransferase-like 3 protein level compared with the control group in human aortic valve interstitial cells. Functionally, methyltransferase-like 3 acted as a positive regulator of osteogenic differentiation of human aortic valve interstitial cells. Mechanistically, methylated RNA immunoprecipitation quantitative reverse-transcription polymerase chain reaction identified twist-related protein 1 as a target of methyltransferase-like 3–mediated m^{6}A modification. Moreover, N6-methyladenosine–mediated twist-related protein 1 mRNA inhibition relied on the m^{6}A binding protein YTH-domain family member 2–dependent pathway.

Conclusions: Methyltransferase-like 3 promotes osteogenic differentiation of human aortic valve interstitial cells by inhibiting twist-related protein 1 through an N6-methyladenosine YTH-domain family member 2–dependent pathway. Our findings provide novel mechanistic insights into a critical role of methyltransferase-like 3 in the aortic valve calcification progression and shed new light on N6-methyladenosine–directed diagnostics and therapeutics in aortic valve calcification. (J Thorac Cardiovasc Surg 2021;161:e163-85)
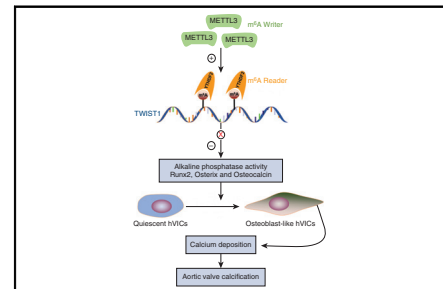
Promotion of AVC by METTL3-mediated m^{6}A modification.

Central Message

METTL3 overexpression is linked with AVC. METTL3 promotes osteogenic differentiation of hVICs via suppressing TWIST1 expression through an m^{6}A-YTHDF2–dependent pathway.

Perspective

hVICs redifferentiate to osteoblast-like phenotype, which is the key cellular mechanism of AVC. This study confirms METTL3 as a positive regulator of hVIC osteogenic differentiation via suppressing TWIST1 expression through an m^{6}A-YTHDF2–dependent pathway, provides novel mechanistic insights into a critical role of METTL3 in AVC, and sheds new light on m^{6}A-directed diagnostics and therapeutics in AVC.

See Commentaries on pages e187 and e188.

Abbreviations and Acronyms

AAV	= adeno-associated virus
ALP	= alkaline phosphatase
AVC	= aortic valve calcification
CAVS	= calcified aortic valve leaflets
hVIC	= human aortic valve interstitial cell
m^6A	= N6-methyladenosine
MeRIP-qRT-PCR	= methylated RNA immunoprecipitation quantitative reverse transcription-polymerase chain reaction
METTL3	= methyltransferase-like 3
METTL14	= methyltransferase-like 14
qRT-PCR	= quantitative reverse transcription-polymerase chain reaction
RIP-qRT-PCR	= RNA immunoprecipitation quantitative reverse transcription-polymerase chain reaction
Runx2	= runt-related transcription factor 2
siRNA	= small interfering RNA
si-METTL3-1	= small interfering RNA for methyltransferase-like 3
si-METTL3-2	= small interfering RNA for methyltransferase-like 3
TWIST1	= twist-related protein 1

▶ Video clip is available online.

Aortic valve calcification (AVC) is the most common valvular disease with high morbidity and mortality rates.[1] However, limited pharmacologic therapeutic approaches are available to prevent the occurrence and progression of AVC beyond surgical valve replacement. Currently, AVC is recognized as an actively regulated disease process that involves the coordinated actions of resident human valve endothelial cells (hVECs), circulating inflammatory and immune cells, and human aortic valve interstitial cells (hVICs).[2] hVICs, the most abundant cells in the aortic valve, spontaneously undergo phenotypic transdifferentiation into osteoblast-like cells in calcific aortic valve leaflets (CAVS).[3] Thus, strategies to effectively prevent transformation of hVICs by inhibiting osteogenic differentiation may

lead to novel therapeutic interventions to halt the progression of or even reverse AVC.

N6-methyladenosine (m^6A) methylation, the most prevalent post-transcriptional methylated modification, is essential for multiple RNA processing events and disease progression.[4] Generally, m^6A is accomplished by the stable core methyltransferase complex, including methyltransferase-like 3 (METTL3), methyltransferase-like 14 (METTL14), and Wilms' tumor 1-associated protein, and recognized by m^6A-binding proteins (YTH m^6A RNA binding protein 1-3, YTH domain containing 1-2).[5] Emerging studies identified that METTL3-mediated m^6A modification plays a critical role in human cardiovascular diseases, such as cardiac hypertrophy,[6] heart failure,[7] and coronary artery disease.[8] Nevertheless, its biological role in AVC remains uncharacterized. Recently, researchers have confirmed that METTL3-mediated m^6A modification could promote the osteogenic differentiation of the bone mesenchymal stem cells.[4] However, whether METTL3-mediated m^6A modification could regulate the osteogenic differentiation of hVICs needed further investigation.

Twist-related protein 1 (TWIST1), a basic helix-loop-helix transcription factor, was highly expressed by valve progenitors and closely related to human cardiovascular diseases.[9-11] Recently, it has been reported that TWIST1 was lowly expressed in AVC and acted as a negative regulator of hVICs osteogenic differentiation.[12] However, the underlying mechanism by which TWIST1 is regulated requires further study. Increasing evidence indicates a positive correlation between hypomethylation status and TWIST1 level.[13] Nevertheless, whether METTL3-mediated m^6A modification could regulate TWIST1 expression during the hVIC osteogenic differentiation remains unknown.

In this study, we provide the first evidence that METTL3 is upregulated in AVC and acts as a positive regulator of the osteogenic phenotype of hVICs. Mechanistic analysis identified TWIST1 as a target of METTL3-mediated m^6A modification. Notably, METTL3 promoted osteogenic differentiation of hVICs via suppressing TWIST1 expression through an m^6A-YTHDF2–dependent manner. Altogether, these results established a METTL3-mediated m^6A modification of TWIST1 regulatory mechanism in in vitro osteogenic differentiation of hVICs.

MATERIALS AND METHODS

An expanded description of the study methods is available in Appendix E1.

Human Aortic Valve Samples

Human CAVS were obtained from the patients with AVC (n = 50) who underwent aortic valve replacement. Control non-CAVS (n = 50) with

normal echocardiographic analyses were collected from the age-matched patients who underwent heart transplant procedures. All of the studies involving humans were approved by the Ethic Board of Tongji Medical College of Huazhong University of Science and Technology and complied with the Declaration of Helsinki. Informed consent was signed before surgery.

Cell Culture and Treatment

hVICs were isolated from noncalcified aortic valves by the collagenase I digestion method as described previously.[14] Figure E1 shows the identification of hVICs, and Table E1 shows details on patient characteristics. Cells at subcultures 3 to 5 were used in all experiments and incubated with an osteogenic induction medium to stimulate osteogenic differentiation as previously described.[14]

Transfection

Transfection of hVICs was performed as previously described.[15] Specific small interfering RNAs (siRNAs) of METTL3, TWIST1, and YTHDF2 were synthesized by Invitrogen (Carlsbad, Calif), and the sequences are listed in Table E2. Overexpression vector targeting METTL3, TWIST1, YTHDF1, YTHDF2, and a negative control empty vector plasmid were purchased from RiboBio (Guangzhou, China).

M^{6}A-RNA Immunoprecipitation Quantitative Reverse-Transcription Polymerase Chain Reaction Assay

Methylated RNA immunoprecipitation quantitative reverse-transcription polymerase chain reaction (MeRIP-qRT-PCR) was performed as previously described.[16] Briefly, after transfection with METTL3 siRNA and stimulation with osteogenic medium for 7 days, hVICs were collected for RNA extraction. Then, chemically fragmented RNA (~100 nt) was incubated with m^{6}A antibody (Merck Millipore, Billerica, Mass) for immunoprecipitation according to the manufacturer's instructions of the Magna MeRIP m^{6}A Kit (EMD Millipore). Finally, quantitative reverse-transcription polymerase chain reaction (qRT-PCR) was used to analyze the enrichment of m^{6}A containing mRNA.

Luciferase Reporter Assay

Luciferase reporter assay was performed as described previously.[16] Briefly, pmirGlo luciferase expression vector from Promega (Madison, Wis) was used to construct the reporter plasmid. The full-length of TWIST1 transcript was inserted after the firefly luciferase coding sequence to make a wild-type TWIST1 reporter plasmid, and we constructed the mutant TWIST1 reporter plasmid through replacing the adenosine bases within the m^{6}A consensus sequences (RRACU) to cytosine (Figure E2). hVICs were assayed with Dual-Glo luciferase system (Promega) after transfection with 500 ng of wild-type and mutated firefly luciferase TWIST1 fusion reporter plasmid for 48 hours. The transfection efficiency of the reporter plasmid was normalized by the Renilla luciferase.

RNA Immunoprecipitation Quantitative Reverse-Transcription Polymerase Chain Reaction Assay

RNA immunoprecipitation quantitative reverse-transcription polymerase chain reaction (RIP-qRT-PCR) assay was performed as described.[17] Briefly, DYDDDDK peptide (FLAG)-YTHDF1 or (FLAG)-YTHDF2 transfected hVICs were lysed in lysis buffer containing murine RNase inhibitor, and protease inhibitor cocktail, YTHDF2 antibody, or rabbit immunoglobulin G was incubated with magnetic beads in lysis buffer for 1.5 hours at 4°C. RNA was extracted from RNA-protein complexes, bound to the beads, and used for qRT-PCR analysis.

Statistical Analysis

The Statistical Package for the Social Sciences 18.0 (IBM-SPSS Inc, Armonk, NY) was used for statistical analysis. Continuous data were presented as means ± standard deviation. The normality of distribution of all continuous variables was confirmed by the Kolmogorov–Smirnov test and visualized by Q-Q plot. Student t test was applied for comparison between 2 groups, and analysis of variance followed by Bonferroni's test was performed when more than 2 groups were compared. Two-tailed Pearson's correlation analysis was used to analyze the association of the 2 variables. For the human study and the in vitro assays with hVICs, n represents the number of experiments performed in different donors (biological replicates).

Sample Size Estimation

Stata software version 12.0 (StataCorp LP, College Station, Tex) was used to estimate the sample size for 2-sample comparison of mean in the human study. The power was set as 0.8, and alpha was set as 0.05. The sample size was set as identical in 2 groups. Results were presented as mean ± standard deviation in the human study.

RESULTS

Methyltransferase-Like 3 Is Upregulated in Human Calcified Aortic Valves

The m^{6}A modification was co-transcriptionally installed on mRNA by a hetero complex of METTL3 and METTL14, assisted by Wilms' tumor 1-associated protein.[18] To explore which component is altered in AVC, we first collected human calcified (n = 50) and control noncalcified (n = 50) aortic valves (Table E3 shows details on patient characteristics), which were confirmed by both Alizarin Red and Von Kossa stainings (Figure E3). Then qRT-PCR analysis was performed to show that the mRNA level of METTL3, but not the other 2, was significantly increased in CAVS tissues (Figure 1, A and B). Both immunofluorescence staining (Figure 1, C) and Western blot (Figure 1, D) further confirmed the increased METTL3 protein level in human CAVS. Collectively, our data demonstrated that METTL3 is upregulated in AVC.

Methyltransferase-Like 3 Is Associated With Osteogenic Differentiation of Human Aortic Valve Interstitial Cells

Because hVICs undergo phenotypic transdifferentiation into osteoblast-like cells in AVC,[3] we further investigated whether METTL3 was associated with hVIC osteogenic differentiation. First, a high level of METTL3 protein was confirmed in hVICs compared with several cell lines, including U937 monocytic cells and primary hVECs (Figure 2, A). Moreover, METTL3 was localized predominantly in the nucleus (Figure 2, B). Next, we incubated hVICs with osteogenic medium for 7 days to stimulate osteogenic differentiation as previously described.[15] The results showed that the protein levels of 3 known osteogenesis-specific markers (runt-related transcription factor 2 [Runx2], Osterix, and Osteocalcin) were upregulated upon osteogenic induction. Notably, osteogenic
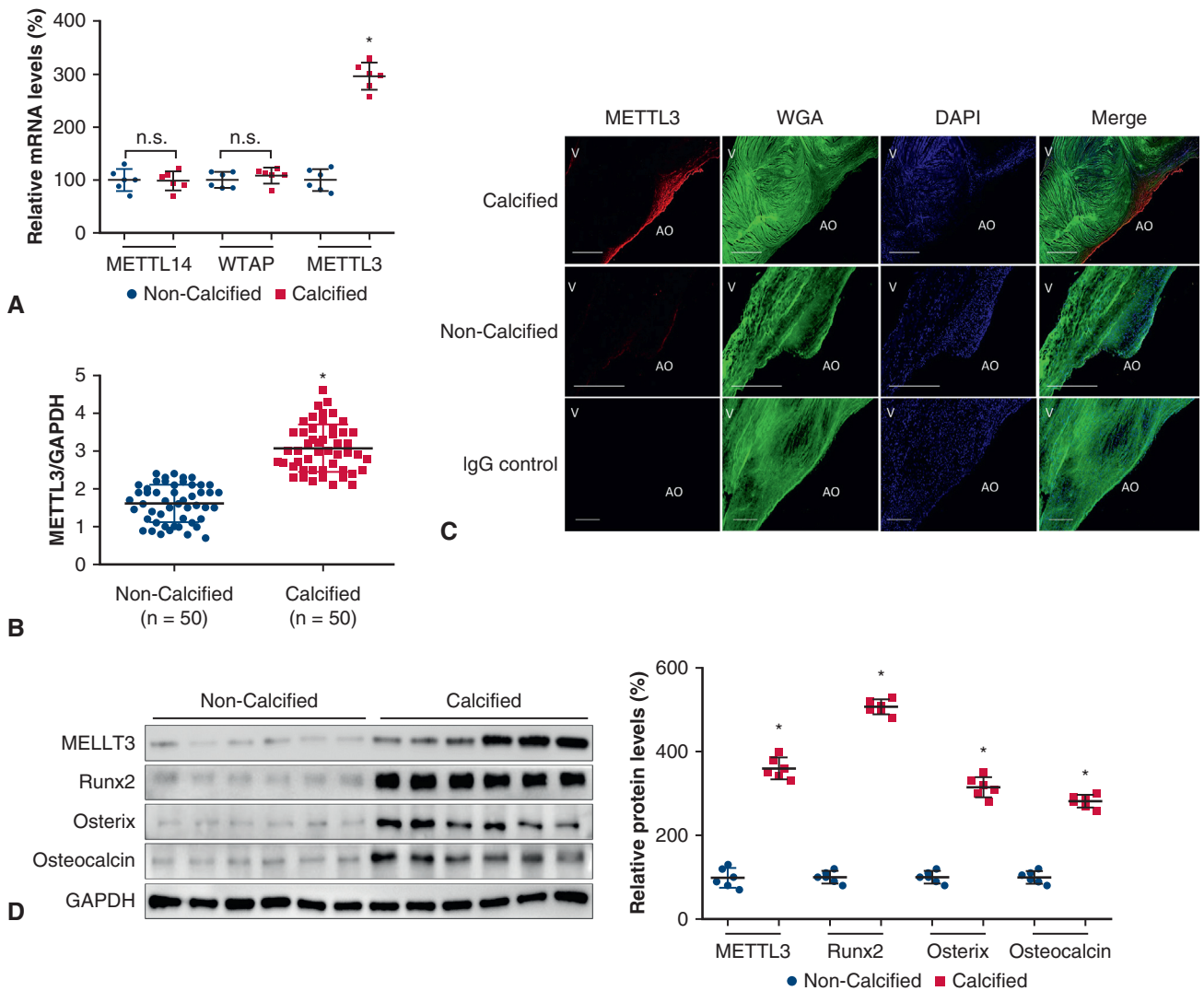
FIGURE 1. METTL3 is highly expressed in human CAVS. A and B, qRT-PCR showed that the mRNA level of METTL3, but not METTL14 and Wilms' tumor 1-associated protein, was increased in human CAVS (n = 50) compared with normal control (n = 50). Increased METTL3 protein level in human CAVS was confirmed by immunofluorescence staining (C) and Western blot (D). The protein levels of METTL3 and 3 osteogenesis-specific markers (Runx2, Osterix, and Osteocalcin) were upregulated in CAVS. Scale bar: 500 μm. *$P < .05$ versus noncalcified control. *n.s.*, Not significant; *DAPI*, 4', 6-diamidino-2-phenylindole; *IgG*, immunoglobulin G; *WGA*, wheat germ agglutinin; *GAPDH*, glyceraldehyde-3-phosphate dehydrogenase.

stimulation for 7 days resulted in a 2.15 ± 0.16-fold increase (Figure 2, C; $P < .0001$) in METTL3 protein level compared with the control group in hVICs. Third, both mRNA and protein levels of METTL3 exhibited a time-dependent gradual increase in hVICs after osteogenic induction (Figure 2, D and E). Finally, there was a strong positive correlation between the mRNA levels of METTL3 and the osteogenesis-specific markers (Runx2, r = 0.5423, $P = .0002$; Osterix, r = 0.5788, $P = .0001$; Osteocalcin, r = 0.5506, $P = .0002$) (Figure 2, F). Thus, METTL3 is associated with osteogenic differentiation of hVICs in AVC.

Methyltransferase-like 3 Promotes Osteogenic Differentiation of Human Valvular Interstitial Cells

We next applied gain- and loss-of-function experiments to confirm whether METTL3 plays a role in AVC. Successful knockdown and overexpression of METTL3 were confirmed by qRT-PCR and Western blot, respectively (Figure E4, A-D). The results showed that siRNA-mediated METTL3 silencing significantly suppressed the osteogenic medium-induced increase in alkaline phosphatase (ALP) activities (Figure 3, A), calcified nodule formation (Figure 3, B), and protein levels of 3 osteogenesis-specific markers (Runx2, Osterix, and
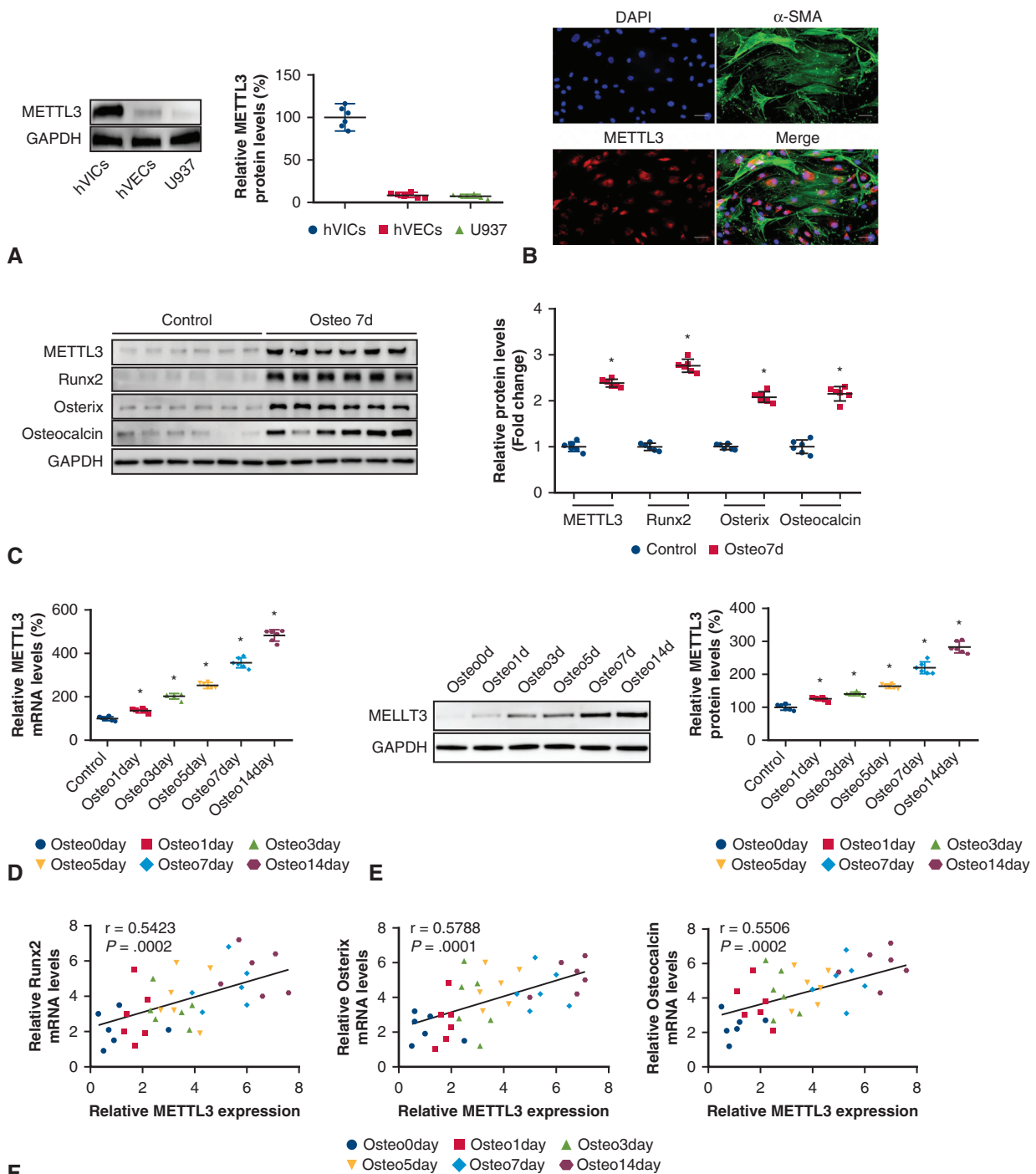
FIGURE 2. METTL3 is associated with osteogenic differentiation of hVICs. A, METTL3 protein level was increased in hVICs compared with cell line U937 and primary hVECs. B, Immunofluorescence staining showed that hVICs were positive for both alpha smooth muscle actin and METTL3. C, Increased protein levels of METTL3 and 3 osteogenesis-specific markers (Runx2, Osterix, and Osteocalcin) in hVICs after osteogenic induction. Both mRNA (D) and protein (E) levels of METTL3 exhibited a time-dependent gradual increase after osteogenic induction in hVICs. F, METTL3 mRNA level was positively correlated with the expression of osteogenesis-specific markers (Runx2, Osterix, Osteocalcin). Scale bar: 50 μm. *P < .05 versus control. *GAPDH*, Glyceraldehyde-3-phosphate dehydrogenase; *DAPI*, 4′, 6-diamidino-2-phenylindole; *α-SMA*, Alpha smooth muscle actin; *Osteo*, osteogenic induction.
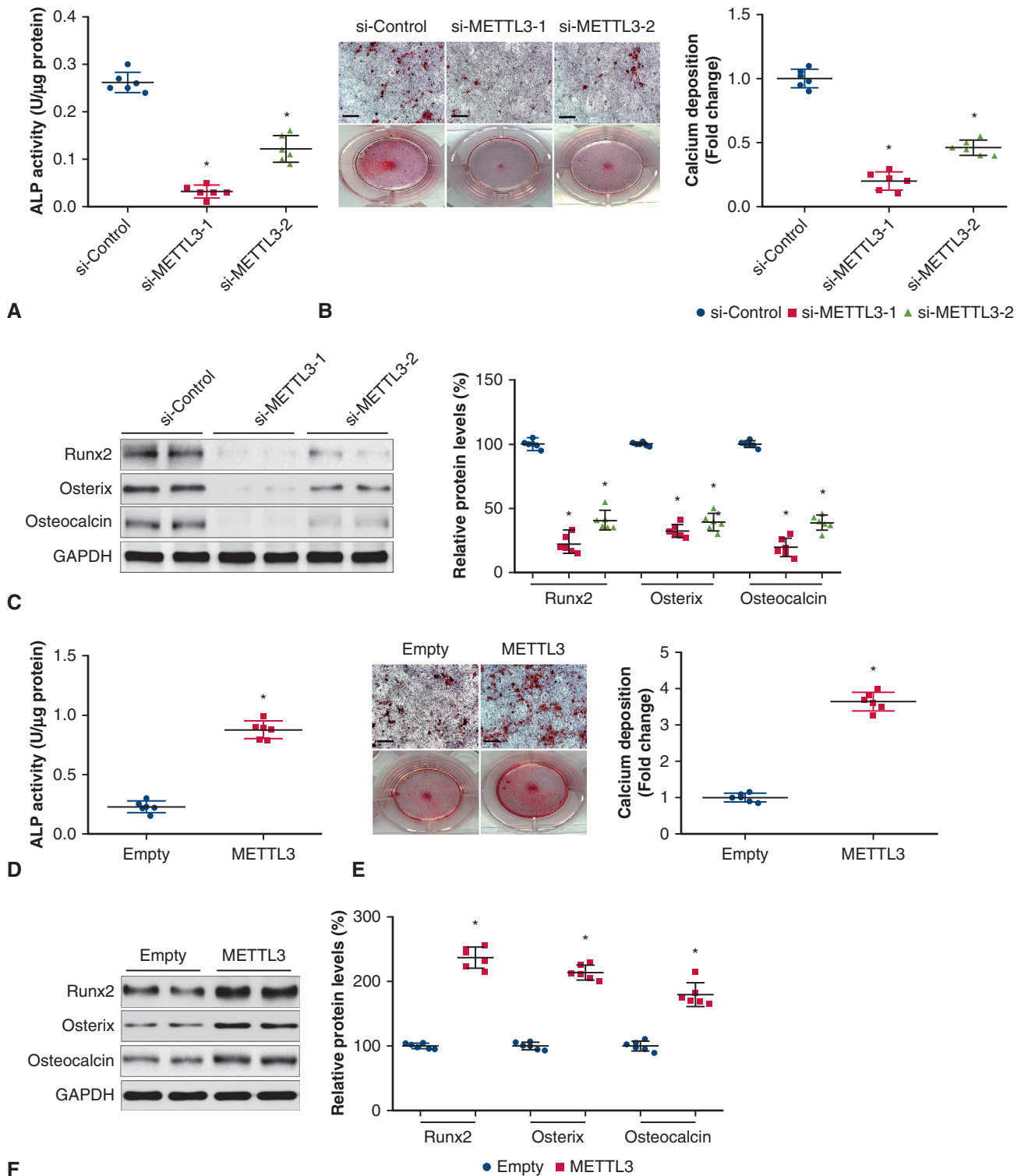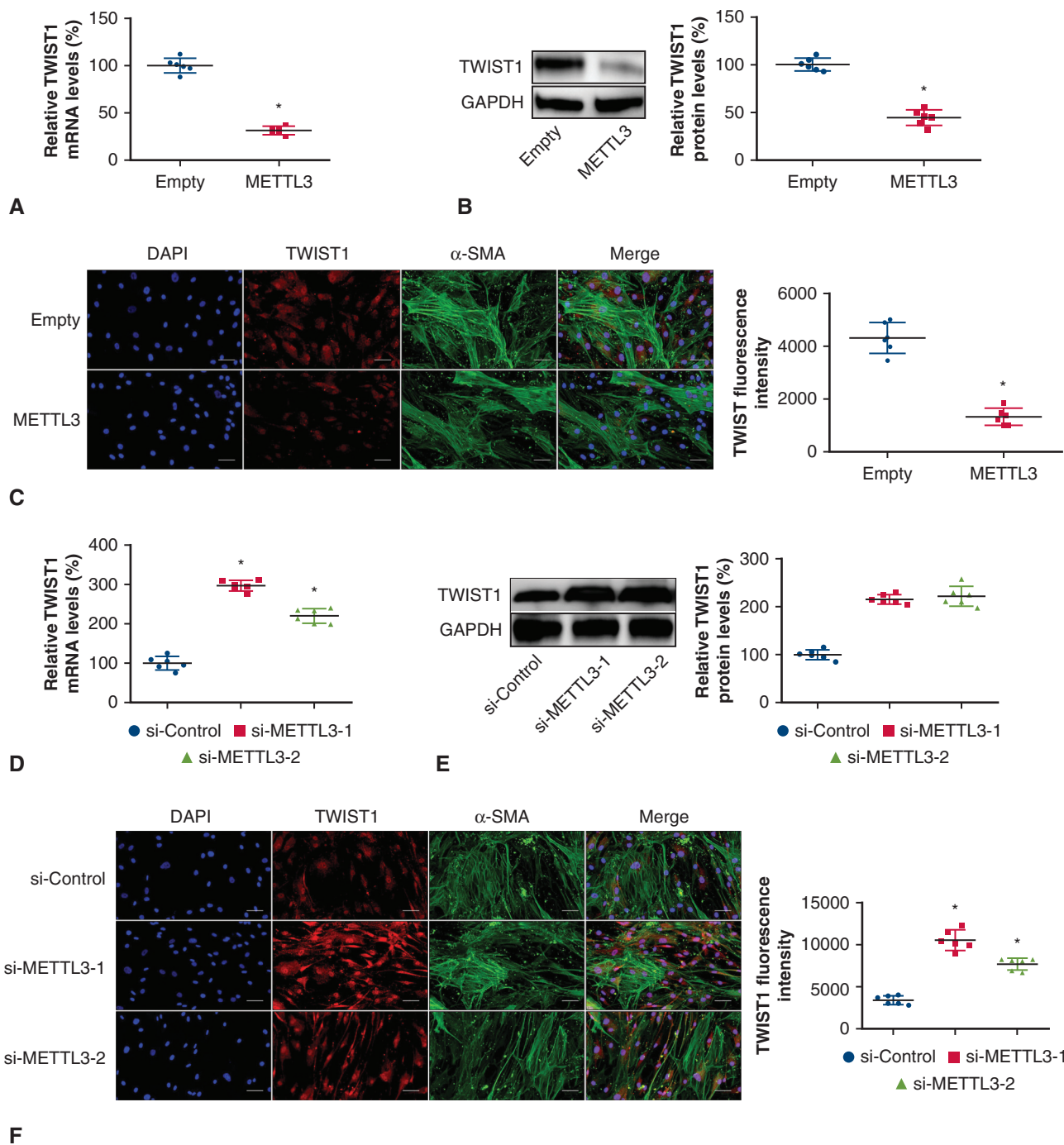
FIGURE 3. METTL3 promotes osteogenic differentiation of hVICs. METTL3 knockdown in hVICs significantly attenuated the osteogenic medium-induced increase in ALP activities (A), calcified nodule formation (B), and protein levels of 3 osteogenesis-specific markers (Runx2, Osterix, and Osteocalcin) (C). METTL3 overexpression in hVICs promoted the osteogenic medium-induced increase in ALP activities (D), calcified nodule formation (E), and protein levels of osteogenesis-specific markers) (F). Scale bar: 50 μm. *P < .05 versus control or empty. *GAPDH*, Glyceraldehyde-3-phosphate dehydrogenase; *si-Control*, small interfering RNA for control; *Empty*, empty vector; *si-METTL3-1*, small interfering RNA 1 for methyltransferase-like 3; *si-METTL3-2*, small interfering RNA 2 for methyltransferase-like 3.

FIGURE 4. METTL3 promotes osteogenic differentiation of hVICs by targeting TWIST1. METTL3 silencing significantly increased the mRNA (A) and protein (B and C) levels of TWIST1. Overexpression of METTL3 decreased the mRNA (D) and protein (E and F) levels of TWIST1. Knockdown of TWIST1 could partially reverse METTL3 silencing-induced decrease in ALP activities (G), calcified nodule formation (H), and protein levels of osteogenesis-specific markers (Runx2, Osterix, and Osteocalcin) (I). Scale bar: 50 μm. *P < .05 versus si-control or empty. #P < .05 versus si-METTL3-1. *Empty*, Empty vector; *DAPI*, 4′, 6-diamidino-2-phenylindole; *α-SMA*, alpha smooth muscle actin; *GAPDH*, glyceraldehyde-3-phosphate dehydrogenase; *si-Control*, small interfering RNA for control; *si-METTL3-1*, small interfering RNA (for methyltransferase-like 3; *si-METTL3-2*, small interfering RNA for methyltransferase-like 3; *si-TWIST1*, small interfering RNA for twist-related protein 1.
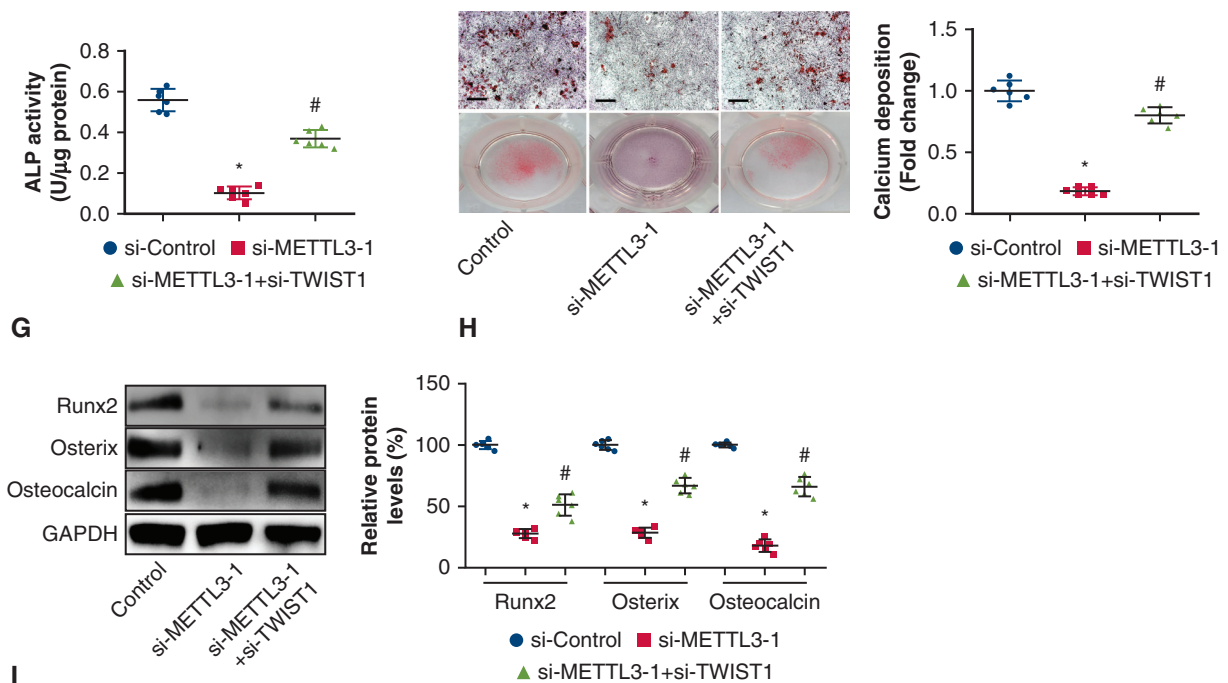
FIGURE 4. Continued

Osteocalcin) (Figure 3, C). In contrast, ALP activity (0.28 ± 0.05 U/μg vs 0.88 ± 0.07 U/μg; P < .0001) (Figure 3, D) was significantly increased in METTL3 overexpression group compared with the empty vector group. Moreover, METTL3 overexpression resulted in a 3.64 ± 0.26-fold increase (P < .0001; Figure 3, E) in calcified nodule formation compared with the empty vector group. METTL3 overexpression resulted in further increases in the protein levels of osteogenesis-specific markers (Figure 3, F). We also found that the diseased interstitial cells behave similarly to the healthy interstitial cells in terms of METTL3 (Figure E5, A-F). Taken together, these results provide concrete evidence that METTL3 plays a positive role in the osteogenic differentiation of hVICs.

Methyltransferase-Like 3 Promotes Osteogenic Differentiation of Human Valvular Interstitial Cells by Targeting Twist-Related Protein 1

We investigated the precise mechanisms by which METTL3 promotes hVIC osteogenic differentiation in AVC. To explore which mRNA contributes to METTL3-mediated positive effects on the osteogenic differentiation of hVICs, we chose 7 crucial factors in AVC (TWIST1,[12] serotonin 2B receptor,[19] Klotho,[20] histone deacetylase 6,[21] calponin 2,[22] cyclooxygenase 2,[23] dipeptidyl peptidase-4[24]) and found that TWIST1 mRNA and protein levels, but not the other 6, were decreased upon METTL3 overexpression (Figure 4, A-C, and Figure E6, A-F). In contrast, METTL3 silencing resulted in an increase in the mRNA

and protein levels of TWIST1 (Figure 4, D-F). Moreover, we also found a negative correlation between the mRNA levels of TWIST1 and METTL3 among human calcific aortic valves (r = −0.4130, P = .003) (n = 50; Figure E7).

Thus, we hypothesize that TWIST1 might be a target of METTL3 during the osteogenic differentiation process of hVICs. To test this hypothesis, we performed in vitro gain- and loss-of-function experiments in hVICs and found that knockdown of TWIST1 (Figure E8) could partially reverse METTL3 silencing-induced decreases in ALP activities (Figure 4, G), calcified nodule formation (Figure 4, H), and protein levels of osteogenesis-specific markers (Runx2, Osterix, and Osteocalcin) (Figure 4, I). These results confirmed that METTL3 promotes osteogenic differentiation of hVICs via suppressing TWIST1 expression.

Methyltransferase-Like 3 Regulates the Expression of Twist-Related Protein 1 Through an m⁶A-YTHDF2–Dependent Pathway

We further explored the precise mechanisms by which METTL3 modulated TWIST1 expression. The observation that METTL3 targets TWIST1 mRNA for m^6A modification was further confirmed by MeRIP-qRT-PCR. As shown in Figure 5, A, compared with the immunoglobulin G pull-down control, the TWIST1 mRNA was significantly enriched by m^6A-specific antibody and the m^6A levels of TWIST1 mRNA were decreased when METTL3 was interfered. To further confirm the effect of METTL3-mediated
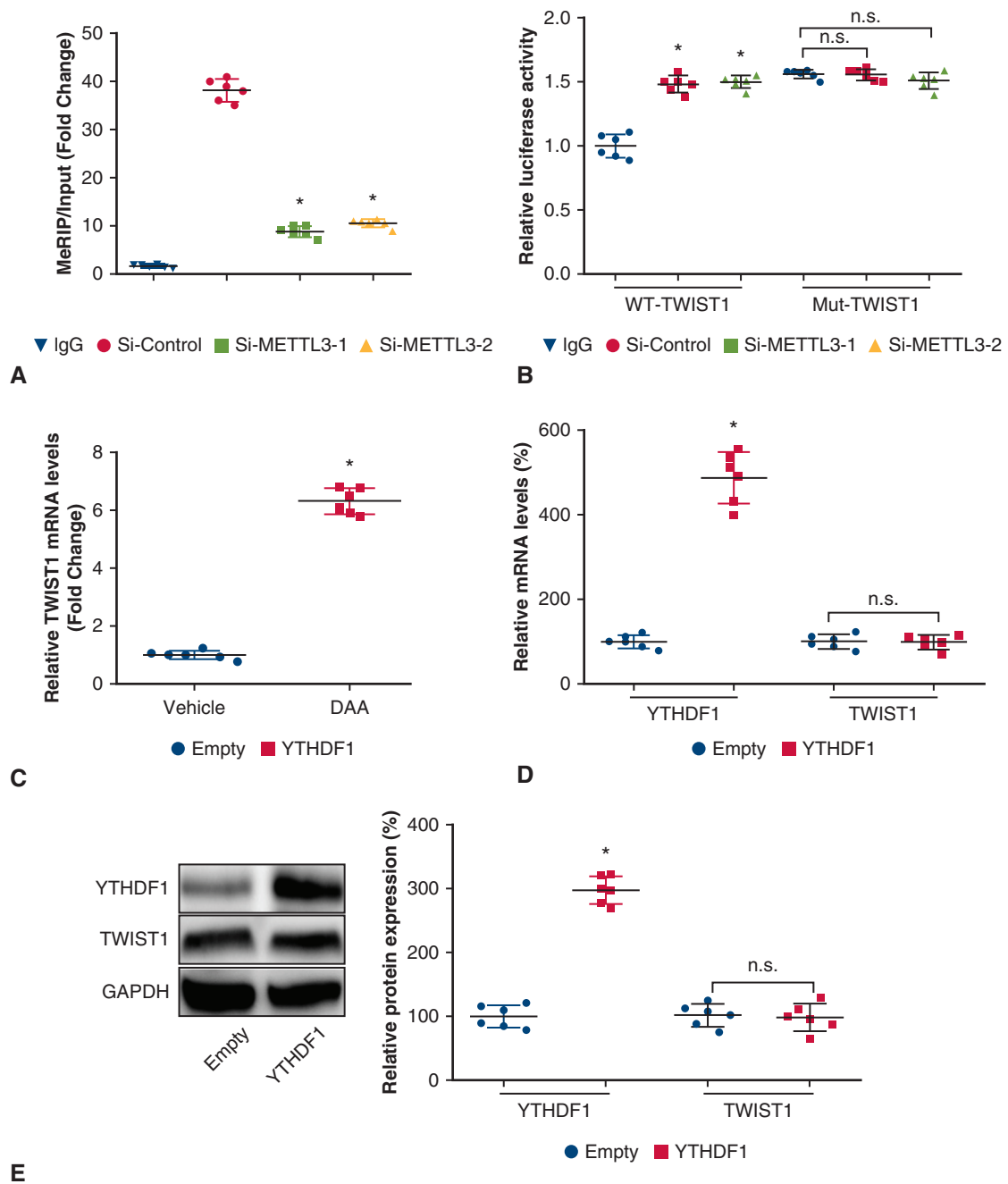
FIGURE 5. METTL3 inhibits TWIST1 expression through an m[6]A-YTHDF2-dependent manner. A, MeRIP-qRT-PCR showed that METTL3 silencing decreased m[6]A levels of TWIST1 mRNA. B, Luciferase reporter assays indicated a specific inhibitory effect of METTL3 on TWIST1. C, 3-deazaadenosine treatment strengthens TWIST1 mRNA levels in hVICs. YTHDF1 overexpression had a minimal effect on mRNA (D) and protein (E) levels of TWIST1. Both mRNA (F) and protein (G) levels of TWIST1 were significantly decreased upon YTHDF2 overexpression hVICs. H, RIP-qRT-PCR revealed that TWIST1 mRNA directly interacted with YTHDF2 protein. I-J, YTHDF2 knockdown upregulated the TWIST1 mRNA expression in hVICs. YTHDF2 silencing could partially reverse METTL3 overexpression-induced decrease in mRNA (K) and protein (L) levels of TWIST1 and increase in ALP activities (M) and calcified nodule formation (N). Scale bar: 50 μm. *$P < .05$ versus control. #$P < .05$ versus METTL3. *IgG*, Immunoglobulin G; *si-METTL3-1*, small interfering RNA for methyltransferase-like 3; *si-METTL3-2*, small interfering RNA for methyltransferase-like 3; *n.s.*, not significant; *si-Control*, small interfering RNA for control; *Empty*, empty vector; *GAPDH*, glyceraldehyde-3-phosphate dehydrogenase; *si-YTHDF2*, small interfering RNA for YTH-domain family member 2.
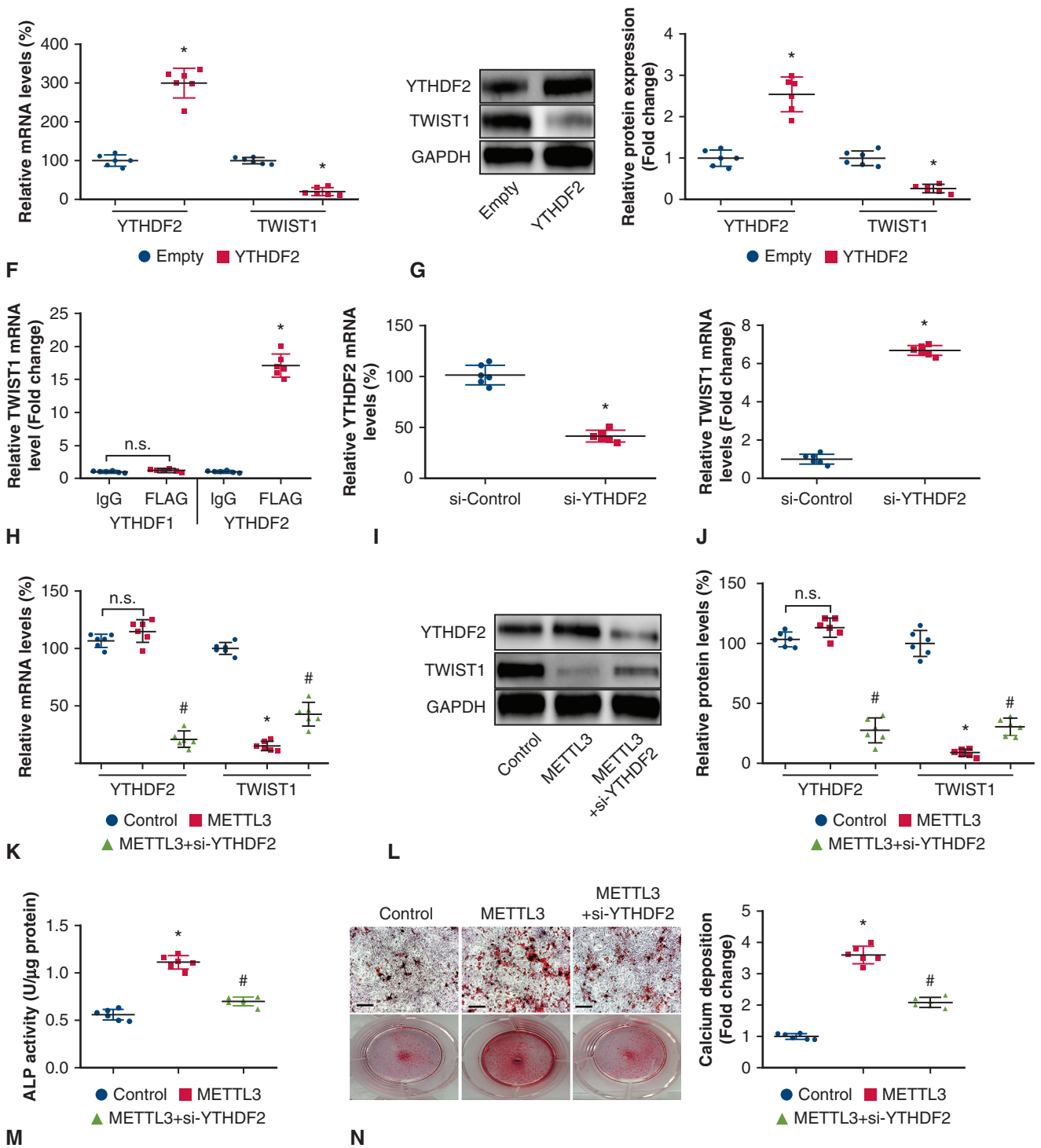
FIGURE 5. Continued

m6A modification on TWIST1 expression, both wild-type and mutant TWIST1 reporter minigenes were constructed. For the mutant form of TWIST1, cytosine was used to replace adenosine bases in m6A consensus sequences (RRACU), thus abolishing m6A modification (Figure E2).

As shown in Figure 5, B, relative luciferase activity of the wild-type and mutant TWIST1 fused reporter was compared in hVICs upon METTL3 silencing. Silencing of METTL3 significantly increased the luciferase activity of the wild-type TWIST1-fused reporter, whereas it had no

FIGURE 6. Graphical abstract of how METTL3-mediated m^{6}A modification promotes AVC. METTL3 promotes osteogenic differentiation of hVICs by inhibiting TWIST1 through an m^{6}A-YTHDF2–dependent pathway. *hVIC*, Human aortic valve interstitial cell.

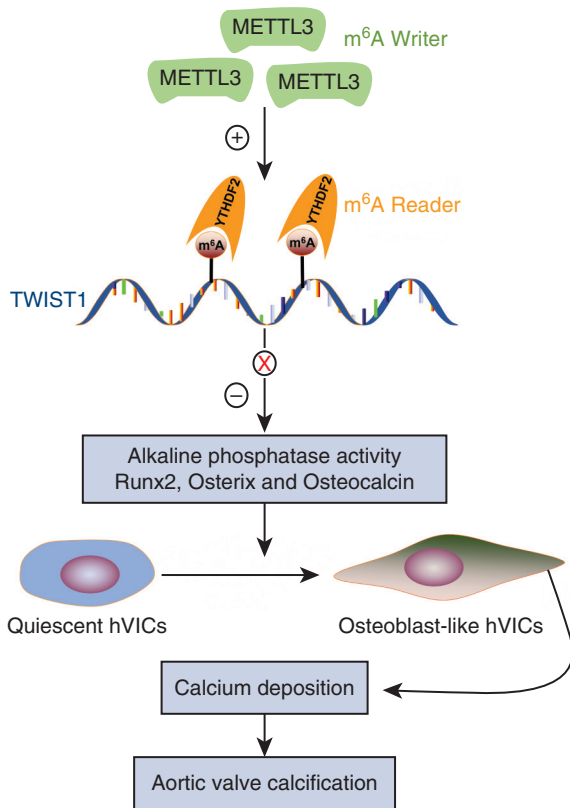effect on the mutant TWIST1-fused reporter. Furthermore, treatment with 3-deazaadenosine, a global methylation inhibitor, resulted in a 6.32 ± 0.45-fold increase ($P < .0001$; Figure 5, *C*) in the TWIST1 mRNA level. Taken together, our results indicated that the modulation of TWIST1 expression is under the control of METTL3-mediated m^{6}A modification in hVICs.

The next question we needed to investigate was how METTL3 regulated the TWIST1 expression. Two m^{6}A "reader" proteins, YTHDF1 and YTHDF2, have been shown to selectively bind to m^{6}A-containing mRNA and accelerate degradation of methylated transcripts,[25] which led us to hypothesize that the m^{6}A-containing TWIST1 mRNA could be selectively bound by YTHDF1 or YTHDF2. To test this hypothesis, both FLAG-tagged YTHDF1and FLAG-tagged YTHDF2 plasmids were constructed. As expected, our results showed that YTHDF1 overexpression had no effects on TWIST1 mRNA and protein levels (Figure 5, *D* and *E*), whereas overexpression of YTHDF2 significantly decreased TWIST1 expression in hVICs (Figure 5, *F* and *G*). Furthermore, RIP-qRT-PCR assay also confirmed that TWIST1 mRNA directly interacted with YTHDF2 protein (Figure 5, *H*). Conversely,
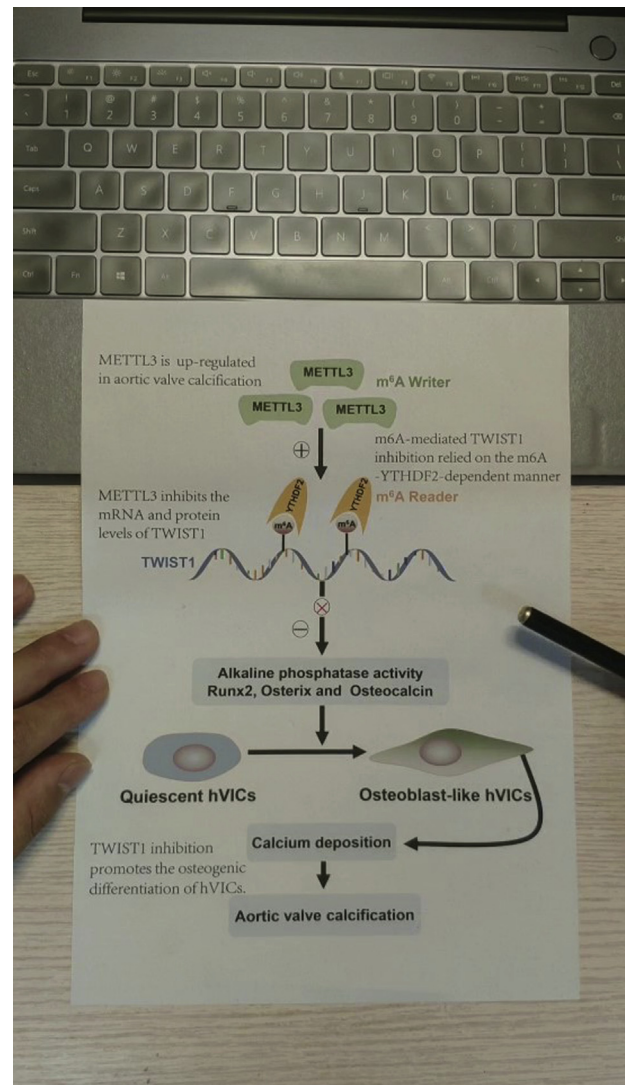
VIDEO 1. Description of the conclusion and significance of the study. In this study, we provide the first evidence that the m^{6}A methylation writer METTL3 is upregulated in AVC and acts as a positive regulator of the osteogenic phenotype of hVICs. Mechanistic analysis revealed that METTL3 targets a transcriptional regulator TWIST1 and inhibits its mRNA and protein levels, and thus promotes the osteogenic differentiation of hVICs. Notably, m^{6}A-mediated TWIST1 inhibition relied on the m^{6}A binding protein YTHDF2-dependent manner. This study established a METTL3-mediated m^{6}A modification of TWIST1 regulatory mechanism in in vitro osteogenic differentiation of hVICs. Our findings provide novel mechanistic insights into the critical role of METTL3 in AVC progression and shed new light on m^{6}A-directed therapeutics in AVC. Video available at: https://www.jtcvs.org/article/S0022-5223(19)32255-X/fulltext.

silencing of YTHDF2 (Figure 5, *I*) resulted in a 6.67 ± 0.26-fold increase ($P < .0001$; Figure 5, *J*) in the TWIST1 mRNA level in hVICs. Finally, we confirmed whether YTHDF2 silencing could partially reverse TWIST1 level and osteogenic differentiation induced by METTL3 in vitro. As expected, knockdown of YTHDF2

partly reversed the upregulation of TWIST1 mRNA and protein levels induced by METTL3 in hVICs (Figure 5, K and L). More important, YTHDF2 silencing efficiently reversed METTL3-mediated increase in ALP activities (Figure 5, M) and calcified nodule formation (Figure 5, N). Taken together, these findings suggested that METTL3 promotes osteogenic differentiation of hVICs through inhibition of TWIST1 via an m^{6}A-YTHDF2-dependent pathway (Figure 6 and Video 1).

DISCUSSION

At present, it is an unmet medical need to discover novel potential therapeutic targets for treating AVC. In this study, our data showed that METTL3, highly expressed in human CAVS and hVICs after osteogenic induction, acts as a positive regulator of osteogenic differentiation of hVICs. Mechanistically, we identified TWIST1 as a target of METTL3-mediated m^{6}A modification. Moreover, m^{6}A-mediated TWIST1 mRNA inhibition relied on the m^{6}A binding protein YTHDF2-dependent pathway. The present study provides the first evidence that METTL3-mediated promotion of hVICs osteogenic differentiation through YTHDF2-dependent silencing of TWIST1 contributes to the progression of AVC.

Although increasing evidence has shown that METTL3-mediated m^{6}A modification plays a crucial role in the pathogenesis of cardiovascular diseases,[6,26] its expression and biological role in AVC remain uncharacterized. In this study, we confirmed for the first time that METTL3, highly expressed in human CAVS, promotes osteogenic differentiation of hVICs, as evidenced by increased ALP activities, calcified nodule formation, and protein levels of 3 osteogenesis-specific markers (Runx2, Osterix, and Osteocalcin). Recently, delivery of miR-199a through an adeno-associated virus (AAV) vector has been shown to induce uncontrolled cardiac repair after myocardial infarction in pigs.[27] Furthermore, the safety of gene therapy through infusion of AAV1 in patients with heart failure and reduced ejection fraction has been confirmed by previous research.[28] Thus, delivery of METTL3 inhibitors through an AAV vector may provide a novel and promising gene therapy approach to AVC treatment in patients. A previous study has uncovered the regulation of m^{6}A RNA methylation by noncoding RNA in cell reprogramming.[29] Our study only revealed an increased METTL3 level in human CAVS and hVICs after osteogenic induction. However, whether its upstream induction mechanisms were involved with noncoding RNA-mediated regulation still needs to be explored. It has been widely recognized that endothelial injury[30] and macrophage activation[31] also contribute to the crucial cellular mechanisms of AVC progression. Thus, whether METTL3 could not only regulate hVICs osteogenic differentiation but also modulate other cellular processes requires further study.

TWIST1 has been reported to play critical roles in human cardiovascular diseases, such as atherosclerosis,[9] pulmonary hypertension,[10] and dilated cardiomyopathy.[11] Although several lines of evidence identify TWIST1 as a negative regulator of hVICs osteogenic differentiation,[12] its upstream induction mechanisms in AVC remain largely unknown. In the present study, our in vitro data confirmed, for the first time, that TWIST1 is directly regulated by METTL3-mediated m^{6}A modification. In fact, TWIST1 has been reported to be modulated by DNA methylation modification during the osteogenic differentiation of MSCs.[13] Another previous study established a role for the histone methyltransferase G9A in the regulation of TWIST1.[32] Thus, whether TWIST1 could be regulated by other methylation modifications in AVC progression needs future investigations. The YT521-B homology (YTH) domains, including YTH domain family 1-3 and YTH domain containing 1-2, also known as m^{6}A "readers," selectively bind m^{6}A-methylated mRNA and control RNA expressions.[33] Our study demonstrated that TWIST1 mRNA directly interacted with YTHDF2 protein and its expression was repressed by METTL3-mediated m^{6}A modification through a YTHDF2-dependent pathway, which corresponded well with a previous study.[16] However, whether other m^{6}A "readers" also play distinct roles in regulation of TWIST1 expression requires further study.

Study Limitations

Our study has several limitations. First, because the methyltransferase complex is composed of several subunits, including RNA binding motif protein 15/15B, Vir-like m^{6}A methyltransferase associated, zinc finger CCCH-type containing 13, and methyltransferase-like 16,[18] whether other subunits also contribute to AVC progression needs to be further explored. Second, only in vitro experiments were conducted in this study to elaborate the role of METTL3 in the osteogenic phenotype of hVICs. Whether METTL3 promotes AVC progression in preclinical animal models still requires further investigation. Third, we only established a METTL3-mediated m^{6}A modification of TWIST1 regulatory mechanism in hVIC osteogenic differentiation. Whether other pathways could also regulate TWIST1 expression needs to be explored. Nonetheless, the present finding in aortic tissues and cell assays exemplified the crucial role of METTL3-mediated m^{6}A modification in AVC.

CONCLUSIONS

In the present study, we demonstrated that METTL3 promotes osteogenic differentiation of hVICs by inhibiting TWIST1 through an m^{6}A-YTHDF2–dependent pathway. Our findings provide novel mechanistic insights into the critical role of METTL3 in AVC progression and shed

new light on m⁶A-directed diagnostics and therapeutics in AVC.

Conflict of Interest Statement

Authors have nothing to disclose with regard to commercial support.

References

1. Deutsch MA, Gummert JF. Intraleaflet hemorrhage and iron-dependent pathomechanisms in calcific aortic valve disease: epiphenomenon or major actor? *J Am Coll Cardiol*. 2019;73:1055-8.
2. Towler DA. Molecular and cellular aspects of calcific aortic valve disease. *Circ Res*. 2013;113:198-208.
3. Yu C, Li L, Xie F, Guo S, Liu F, Dong N, et al. LncRNA TUG1 sponges miR-204-5p to promote osteoblast differentiation through upregulating Runx2 in aortic valve calcification. *Cardiovasc Res*. 2018;114:168-79.
4. Wu Y, Xie L, Wang M, Xiong Q, Guo Y, Liang Y, et al. Mettl3-mediated m(6)A RNA methylation regulates the fate of bone marrow mesenchymal stem cells and osteoporosis. *Nat Commun*. 2018;9:4772.
5. Wang X, Feng J, Xue Y, Guan Z, Zhang D, Liu Z, et al. Structural basis of N(6)-adenosine methylation by the METTL3-METTL14 complex. *Nature*. 2016;534:575-8.
6. Dorn LE, Lasman L, Chen J, Xu X, Hund TJ, Medvedovic M, et al. The N(6)-methyladenosine mRNA methylase METTL3 controls cardiac homeostasis and hypertrophy. *Circulation*. 2019;139:533-45.
7. Mathiyalagan P, Adamiak M, Mayourian J, Sassi Y, Liang Y, Agarwal N, et al. FTO-dependent N(6)-methyladenosine regulates cardiac function during remodeling and repair. *Circulation*. 2019;139:518-32.
8. Mo XB, Lei SF, Zhang YH, Zhang H. Detection of m(6)A-associated SNPs as potential functional variants for coronary artery disease. *Epigenomics*. 2018;10:1279-87.
9. Mahmoud MM, Kim HR, Xing R, Hsiao S, Mammoto A, Chen J, et al. TWIST1 integrates endothelial responses to flow in vascular dysfunction and atherosclerosis. *Circ Res*. 2016;119:450-62.
10. Mammoto T, Muyleart M, Konduri GG, Mammoto A. Twist1 in hypoxia-induced pulmonary hypertension through transforming growth factor-beta-Smad signaling. *Am J Respir Cell Mol Biol*. 2018;58:194-207.
11. Baumgarten A, Bang C, Tschirner A, Engelmann A, Adams V, von Haehling S, et al. TWIST1 regulates the activity of ubiquitin proteasome system via the miR-199/214 cluster in human end-stage dilated cardiomyopathy. *Int J Cardiol*. 2013;168:1447-52.
12. Zhang XW, Zhang BY, Wang SW, Gong DJ, Han L, Xu ZY, et al. Twist-related protein 1 negatively regulated osteoblastic transdifferentiation of human aortic valve interstitial cells by directly inhibiting runt-related transcription factor 2. *J Thorac Cardiovasc Surg*. 2014;148:1700-8.
13. Marofi F, Vahedi G, Solali S, Alivand M, Salarinasab S, Zadi Heydarabad M, et al. Gene expression of TWIST1 and ZBTB16 is regulated by methylation modifications during the osteoblastic differentiation of mesenchymal stem cells. *J Cell Physiol*. 2019;234:6230-43.
14. Wang Y, Xiao X, Zhou T, Han D, Dong N. Novel mechanisms for osteogenic differentiation of human aortic valve interstitial cells. *J Thorac Cardiovasc Surg*. June 6, 2019 [Epub ahead of print].
15. Xiao X, Zhou T, Guo S, Guo C, Zhang Q, Dong N, et al. LncRNA MALAT1 sponges miR-204 to promote osteoblast differentiation of human aortic valve interstitial cells through up-regulating Smad4. *Int J Cardiol*. 2017;243:404-12.
16. Chen M, Wei L, Law CT, Tsang FH, Shen J, Cheng CL, et al. RNA N6-methyladenosine methyltransferase-like 3 promotes liver cancer progression through YTHDF2-dependent posttranscriptional silencing of SOCS2. *Hepatology*. 2018;67:2254-70.
17. Yao Y, Bi Z, Wu R, Zhao Y, Liu Y, Liu Q, et al. METTL3 inhibits BMSC adipogenic differentiation by targeting the JAK1/STAT5/C/EBPbeta pathway via an m(6)A-YTHDF2-dependent manner. *FASEB J*. 2019;33:7529-44.
18. Shi H, Wei J, He C. Where, when, and how: context-dependent functions of RNA methylation writers, readers, and erasers. *Mol Cell*. 2019;74:640-50.
19. Hutcheson JD, Ryzhova LM, Setola V, Merryman WD. 5-HT(2B) antagonism arrests non-canonical TGF-beta1-induced valvular myofibroblast differentiation. *J Mol Cell Cardiol*. 2012;53:707-14.
20. Li F, Yao Q, Ao L, Cleveland JC Jr, Dong N, Fullerton DA, et al. Klotho suppresses high phosphate-induced osteogenic responses in human aortic valve interstitial cells through inhibition of Sox9. *J Mol Med*. 2017;95:739-51.
21. Fu Z, Li F, Jia L, Su S, Wang Y, Cai Z, et al. Histone deacetylase 6 reduction promotes aortic valve calcification via an endoplasmic reticulum stress-mediated osteogenic pathway. *J Thorac Cardiovasc Surg*. November 15, 2018 [Epub ahead of print].
22. Plazyo O, Liu R, Moazzem Hossain M, Jin JP. Deletion of calponin 2 attenuates the development of calcific aortic valve disease in ApoE(-/-) mice. *J Mol Cell Cardiol*. 2018;121:233-41.
23. Wirrig EE, Gomez MV, Hinton RB, Yutzey KE. COX2 inhibition reduces aortic valve calcification in vivo. *Arterioscler Thromb Vasc Biol*. 2015;35:938-47.
24. Choi B, Lee S, Kim SM, Lee EJ, Lee SR, Kim DH, et al. Dipeptidyl peptidase-4 induces aortic valve calcification by inhibiting insulin-like growth factor-1 signaling in valvular interstitial cells. *Circulation*. 2017;135:1935-50.
25. Du H, Zhao Y, He J, Zhang Y, Xi H, Liu M, et al. YTHDF2 destabilizes m(6)A-containing RNA through direct recruitment of the CCR4-NOT deadenylase complex. *Nat Commun*. 2016;7:12626.
26. Song H, Feng X, Zhang H, Luo Y, Huang J, Lin M, et al. METTL3 and ALKBH5 oppositely regulate m(6)A modification of TFEB mRNA, which dictates the fate of hypoxia/reoxygenation-treated cardiomyocytes. *Autophagy*. 2019;15:1419-37.
27. Gabisonia K, Prosdocimo G, Aquaro GD, Carlucci L, Zentilin L, Secco I, et al. MicroRNA therapy stimulates uncontrolled cardiac repair after myocardial infarction in pigs. *Nature*. 2019;569:418-22.
28. Greenberg B, Butler J, Felker GM, Ponikowski P, Voors AA, Desai AS, et al. Calcium upregulation by percutaneous administration of gene therapy in patients with cardiac disease (CUPID 2): a randomised, multinational, double-blind, placebo-controlled, phase 2b trial. *Lancet*. 2016;387:1178-86.
29. Chen T, Hao YJ, Zhang Y, Li MM, Wang M, Han W, et al. m(6)A RNA methylation is regulated by microRNAs and promotes reprogramming to pluripotency. *Cell Stem Cell*. 2015;16:289-301.
30. Kostyunin AE, Yuzhalin AE, Ovcharenko EA, Kutikhin AG. Development of calcific aortic valve disease: do we know enough for new clinical trials? *J Mol Cell Cardiol*. 2019;132:189-209.
31. Li G, Qiao W, Zhang W, Li F, Shi J, Dong N. The shift of macrophages toward M1 phenotype promotes aortic valvular calcification. *J Thorac Cardiovasc Surg*. 2017;153:1318-26.
32. Higashihori N, Lehnertz B, Sampaio A, Underhill TM, Rossi F, Richman JM. Methyltransferase G9A regulates osteogenesis via twist gene repression. *J Dent Res*. 2017;96:1136-44.
33. Wang X, Lu Z, Gomez A, Hon GC, Yue Y, Han D, et al. N6-methyladenosine-dependent regulation of messenger RNA stability. *Nature*. 2014;505:117-20.

Key Words: aortic valve calcification, N6-methyladenosine, methyltransferase-like 3, twist-related protein 1, osteogenic differentiation

Cell Culture and Treatments

To isolate hVICs, noncalcified aortic valves were obtained from patients who underwent heart transplant procedures (Table E1 shows details on patient characteristics). Patients with a history of infective endocarditis, rheumatic heart disease, or a genetic syndrome were excluded. Primary hVICs were isolated from noncalcified aortic valves by the collagenase I digestion method as described previously.[E1] Briefly, aortic valves were digested in 1 mg/mL type I collagenase for 30 minutes at 37°C. After endothelial cells were removed by vortex, the leaflets were further incubated with a fresh solution of 1.0 mg/mL collagenase medium for 4 to 6 hours at 37°C. After repeated aspirations to break up the tissue mass, the cell suspension was gently spun for 10 minutes at 1000 rpm to precipitate cells. Finally, isolated VICs were resuspended, seeded, and cultured in Dulbecco's modified Eagle's medium (Gibco, Invitrogen Corporation, Carlsbad, Calif) containing 100 μg/mL streptomycin (Gibco), 10% fetal bovine serum, and 100 U/mL penicillin (Gibco) at 37°C supplied with 5% carbon dioxide atmosphere. Cells at subcultures 3 to 5 were used in all experiments. When grown to 70% to 90% confluence, cells were incubated with an osteogenic induction medium (growth medium supplemented with 50 mg/mL ascorbic acid, 0.1% fetal bovine serum, 5 mmol/L β-glycerophosphate, 50 ng/mL BMP-2, and 100 nmol/L dexamethasone; all purchased from Sigma-Aldrich Ltd, St Louis, Mo)[E2] to stimulate osteogenic differentiation. U937 monocytic cells were purchased from the cell center of Wuhan University and cultured as described previously.[E3] Primary hVECs were isolated from noncalcified aortic valves as described previously.[E4]

Western Blot

Total protein was extracted from the snap-frozen aortic valves and cultured hVICs using RIPA solution (Thermo Fisher, Waltham, Mass) with a protease inhibitor cocktail (Thermo Fisher) according to the manufacturer's instructions. For protein quantification, we use a BCA Protein Assay Kit (Thermo Fisher). Then, 20 μg of total protein of each sample was separated by 10% sodium dodecyl sulfate-polyacrylamide gel electrophoresis and electro blotted onto polyvinylidene difluoride membranes. After blockade with tri-buffered saline containing 5% skim milk and 0.05% Tween 20, membranes were incubated with individual antibodies overnight at 4°C, washed and incubated with the specific horseradish peroxidase–conjugated secondary antibody, and visualized using an enhanced chemiluminescence Western Blotting Kit (Thermo Fisher). Band intensity was analyzed using ImageJ software (National Institutes of Health). The primary antibodies used in this study were anti-METTL3 (15073-1-AP), anti-TWIST1 (25465-1-AP), anti-YTHDF1 (17479-1-AP), anti-YTHDF2 (24744-1-AP), anti-RUNX2 (ab23981), anti-osterix (ab22552), anti-osteocalcin (ab93876), anti-alpha smooth muscle actin (ab5694), anti-vimentin (ab8978), anti-serotonin 2B receptor (19510002), anti-histone deacetylase 6 (ab1440), anti-Klotho (AF1819), anti-glyceraldehyde-3-phosphate dehydrogenase (sc-32233), anti-calponin 2 (21073-1-AP), anti-cyclooxygenase 2 (ab15191), and anti-dipeptidyl peptidase-4 (AF1180).

Quantitative Real-time Polymerase Chain Reaction

qRT-PCR analysis was conducted as previously described.[E2] Total RNA was isolated from human aortic valves and hVICs using Trizol reagent (Invitrogen), and then cDNA synthesized using the PrimeScript RT Reagent Kit (Takara Bio, Otsu, Shiga, Japan). SYBR green polymerase chain reaction reagent (Takara Bio) was used for qRT-PCR using a StepOne Real-Time PCR System (Applied Biosystems, Foster City, Calif). All primers were purchased from Invitrogen, and the sequences are listed in Table E4. Glyceraldehyde-3-phosphate dehydrogenase was used as the internal control.

Transfection

Specific siRNAs of METTL3 (si-METTL3-1,2), TWIST1 (si-TWIST1), and YTHDF2 (si-YTHDF2) and the negative control siRNA with no definite target were purchased from Invitrogen. The siRNAs sequences are listed in Table E2. Transfection was achieved by using Lipofectamine RNAiMax (Thermo Fisher) for siRNA and Lipofectamine 2000 (Thermo Fisher) for plasmid following the manufacturer's protocols. Overexpression vector targeting METTL3, TWIST1, YTHDF1, YTHDF2 and a negative control empty vector plasmid were purchased from RiboBio (Guangzhou, China). After transfection for 48 hours, stable cell lines were selected for further experiments.

M⁶A-RNA Immunoprecipitation Assay

After transfection with METTL3 siRNA and stimulation with osteogenic medium for 7 days, total RNAs were extracted from hVICs and their corresponding nontarget controls using Trizol reagent (Invitrogen, Carlsbad, Calif). To avoid DNA contaminations, RNAs were treated with DNase according to TURBO DNA-freeTM Kit (Thermo Fisher) protocol. MeRIP was performed using the Magna MeRIP m⁶A Kit (EMD Millipore, Billerica, Mass), as described in previous studies.[E5] Briefly, the RNA concentration of each sample was adjusted to 1 μg/μL with nuclease-free water and then chemically fragmented into approximately 100 nt size. Fragmented RNA was then incubated with m⁶A antibody bound-protein A/G magnetic beads in immunoprecipitation buffer for 2 hours at 4°C. Enrichment of m⁶A containing mRNA was then analyzed through

qRT-PCR. For control experiments, m[6]A antibody was replaced by mouse immunoglobulin G.

Alkaline Phosphatase Activity and Alizarin Red Staining in Human Valvular Interstitial Cells

ALP activity was performed as described previously[E1] using ALP colorimetric assay kit (Abcam, Cambridge, UK) by measuring the p-nitrophenol release in absorbance at 405 nm. Results are presented as relative ALP activity normalized to that of the control cells. For Alizarin Red S staining, after treating with a conditioning medium for 21 days, cells were washed twice in phosphate-buffered saline, fixed in 4% formaldehyde for 30 minutes, and stained with 0.2% alizarin red solution. The red staining indicates calcified nodule formation. The stained cells were then incubated for 30 minutes in 10% acetic acid to quantify the calcium deposition, and the absorbance was read at 405 nm with a spectrophotometer.

Immunofluorescence Staining

Immunofluorescence staining was applied for detection of METTL3, TWIST1 in human aortic valve tissues, and hVICs. Briefly, frozen sections (5-μm thick) of aortic valves were fixed in 4% paraformaldehyde for 20 minutes after being dried at room temperature for 15 minutes and then permeabilized with 0.1% Triton X-100 in phosphate-buffered saline for another 20 minutes. Next, tissues were stained as previously described.[E6] The contour of plasma membrane was outlined by using Alexa 488-tagged wheat germ agglutinin (green). For hVICs, at the end of the culture or treatment period, the fixation and immunofluorescence staining were performed as previously described.[E7] Images were taken with a fluorescence microscope (Carl Zeiss, Jena, Germany) and merged using Image Pro-Plus software (Media Cybernetics, Bethesda, Md). The fluorescence intensity was assessed using Image Analysis Software and MetaMorph Microscopy Automation (Molecular Devices, Sunnyvale, Calif).

Von Kossa Staining and Alizarin Red Staining in Human Aortic Valves

Human aortic valves were rinsed in phosphate-buffered saline, fixed in 4% paraformaldehyde, and embedded in paraffin. Then the aortic valves were cut into 3-μm slices and stained with alizarin red.[E2] For Von Kossa staining, paraffin sections were stained with a Von Kossa staining kit (Abcam, Cambridge, UK) according to the manufacturer's instruction.

E-References

E1. Wang Y, Xiao X, Zhou T, Han D, Dong N. Novel mechanisms for osteogenic differentiation of human aortic valve interstitial cells. *J Thorac Cardiovasc Surg.* June 6, 2019 [Epub ahead of print].

E2. Yu C, Li L, Xie F, Guo S, Liu F, Dong N, et al. LncRNA TUG1 sponges miR-204-5p to promote osteoblast differentiation through upregulating Runx2 in aortic valve calcification. *Cardiovasc Res.* 2018;114:168-79.

E3. Li G, Qiao W, Zhang W, Li F, Shi J, Dong N. The shift of macrophages toward M1 phenotype promotes aortic valvular calcification. *J Thorac Cardiovasc Surg.* 2017;153:1318-27.

E4. Choi B, Lee S, Kim SM, Lee EJ, Lee SR, Kim DH, et al. Dipeptidyl peptidase-4 induces aortic valve calcification by inhibiting insulin-like growth factor-1 signaling in valvular interstitial cells. *Circulation.* 2017;135:1935-50.

E5. Chen M, Wei L, Law CT, Tsang FH, Shen J, Cheng CL, et al. RNA N6-methyladenosine methyltransferase-like 3 promotes liver cancer progression through YTHDF2-dependent posttranscriptional silencing of SOCS2. *Hepatology.* 2018;67:2254-70.

E6. Li F, Song R, Ao L, Reece TB, Cleveland JC Jr, Dong N, et al. ADAMTS5 deficiency in calcified aortic valves is associated with elevated pro-osteogenic activity in valvular interstitial cells. *Arterioscler Thromb Vasc Biol.* 2017;37:1339-51.

E7. Xiao X, Zhou T, Guo S, Guo C, Zhang Q, Dong N, et al. LncRNA MALAT1 sponges miR-204 to promote osteoblast differentiation of human aortic valve interstitial cells through up-regulating Smad4. *Int J Cardiol.* 2017;243:404-12.
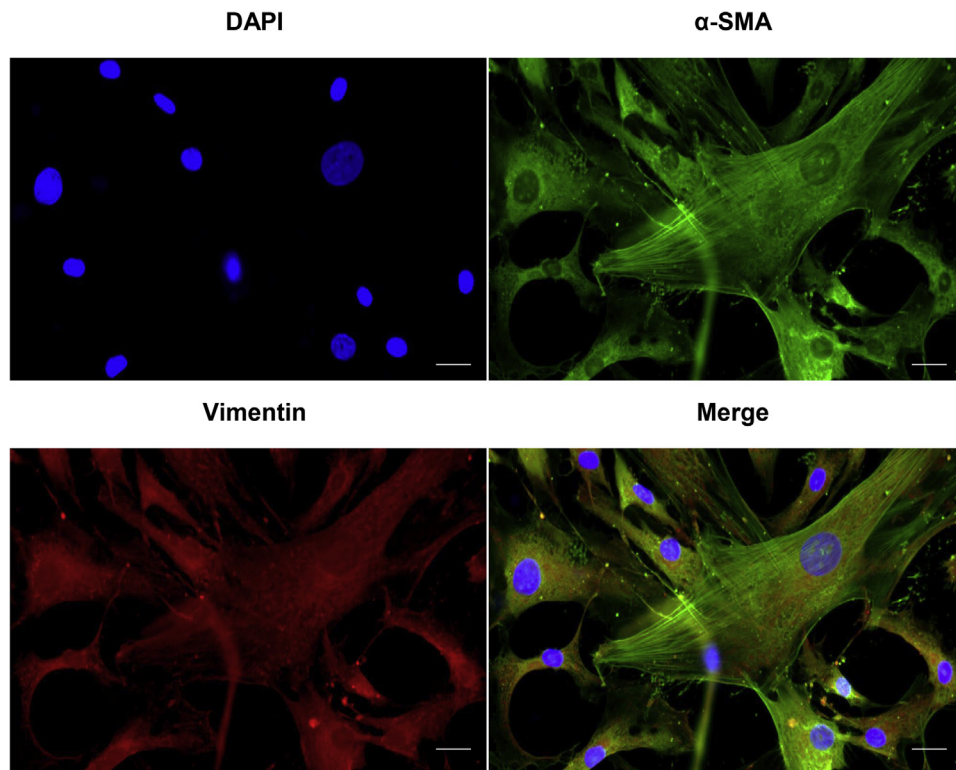
ADULT

FIGURE E1. Immunofluorescence staining showed that hVICs were positive for both alpha smooth muscle actin (*green*) and vimentin (*red*). DAPI was used for nuclear counterstaining (*blue*). Scale bar: 50 μm.

```
  1  CCCUGGCUGCCCCUGUGCCAGGGAACAGGGGCCGGCCUGGGGGCUGGGAGGGCCA   55
 56  GGGGCACCUCCCUCCCACCCUUCAGGCUGCACUGUGUGUGAAGUAGCCACCUGCC  110
111  CUGCCUCCCUCCUCCCCGUUGGCCCCUGUUUGGACUUAGUGCCUGUCUGGCAGCC  165
166  UGUGGGGUCAGGAGAAGCACCCCCAGGGCAGCCCUUGACUGGCGCAGUGGGAA   220
221  GAGGCCUUCAGCCCCUCUCCCGGAGAUGGAAUCGCGGGGCAGGGAGGGGCAGGGU  275
276  GUUCUAGAGGUGAGAAGAGGGCCUGGUGGAGAUUCCCUGUCUUCUGAGCCCGAGC  330
331  CCCUCAUUACCAGUGAAGGACAUGCUUGAGGGGUUCGGGAAGCUCCUCAUCUGAG  385
386  GCAACUGGUCCUGGGGGUGCUCAGGCCUGCCUUUUUGGGACUCAGAUGGCAGGAG  440
441  GUCCACCCCGCAGCCUGGUCCUCGGCUCUCCCACAGGUGGGCACCCCCCACUUUG  495
496  GUGCUAAUAGCUCUCCACCAGGUGGUGUGAGCGCGGGGGCUGCCAGAAGCGGGAG  550
551  GGGUCACUGCCGGAAGAGCAGCUGCCCUCCGACCCCUCACUUUGUGCCUUUAGUA  605
606  AACACUGUGCUUUGUA                                         621
```

m⁶A consensus sequence: 5′-RRACU-3′
(R = A or G; methylated adenosine residue is underscored)

FIGURE E2. Sequence analysis of TWIST1 3′-untranslated region revealed 2 matches to the 5′-RRACU-3′ (methylated adenosine residue is underscored) m⁶A consensus sequence.
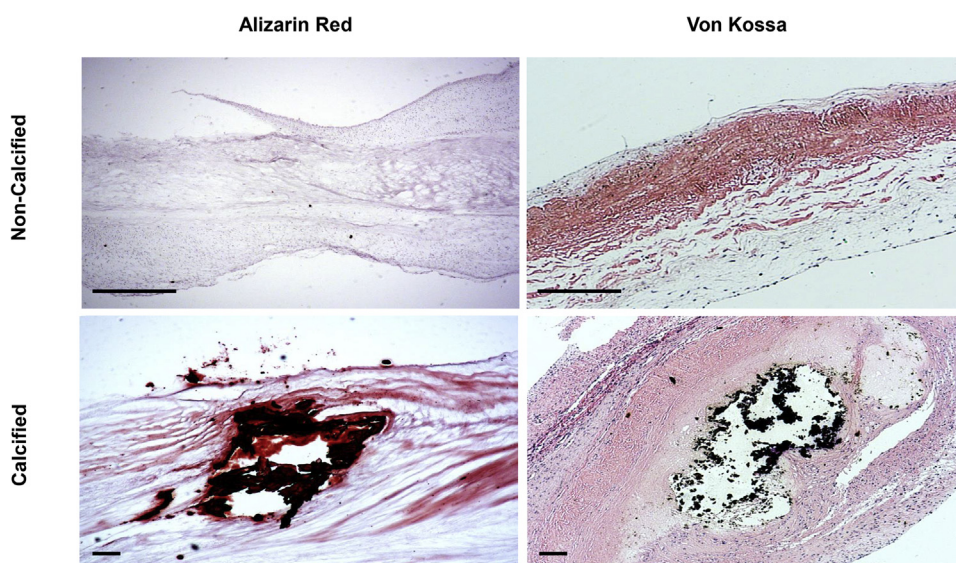

FIGURE E3. Human CAVS were confirmed by both Alizarin Red and Von Kossa stainings. Scale bar: 500 μm.
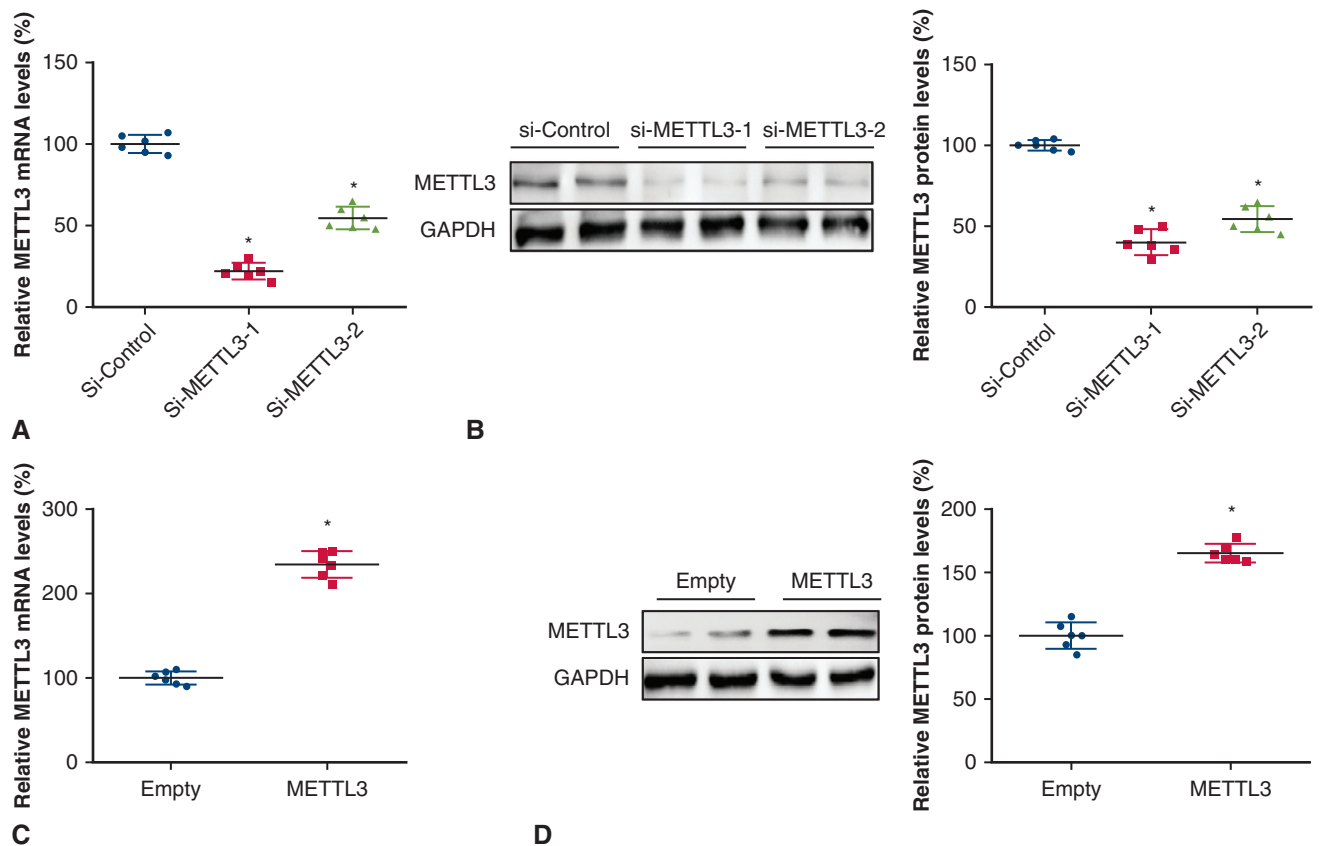
FIGURE E4. The mRNA (A) and protein (B) levels of METTL3 were decreased after silencing of METTL3 with 2 small interfering RNAs (si-METLL3-1 and si-METTL3-2) in hVICs. The mRNA (C) and protein (D) levels of METTL3 were increased after METTL3 overexpression. *$P <$ .05 versus si-control or empty. *si-Control*, Small interfering RNA for control; *si-METTL3-1*, small interfering RNA for methyltransferase-like 3; *si-METTL3-2*, small interfering RNA for methyltransferase-like 3; *Empty*, empty vector; *GAPDH*, Glyceraldehyde-3-phosphate dehydrogenase.
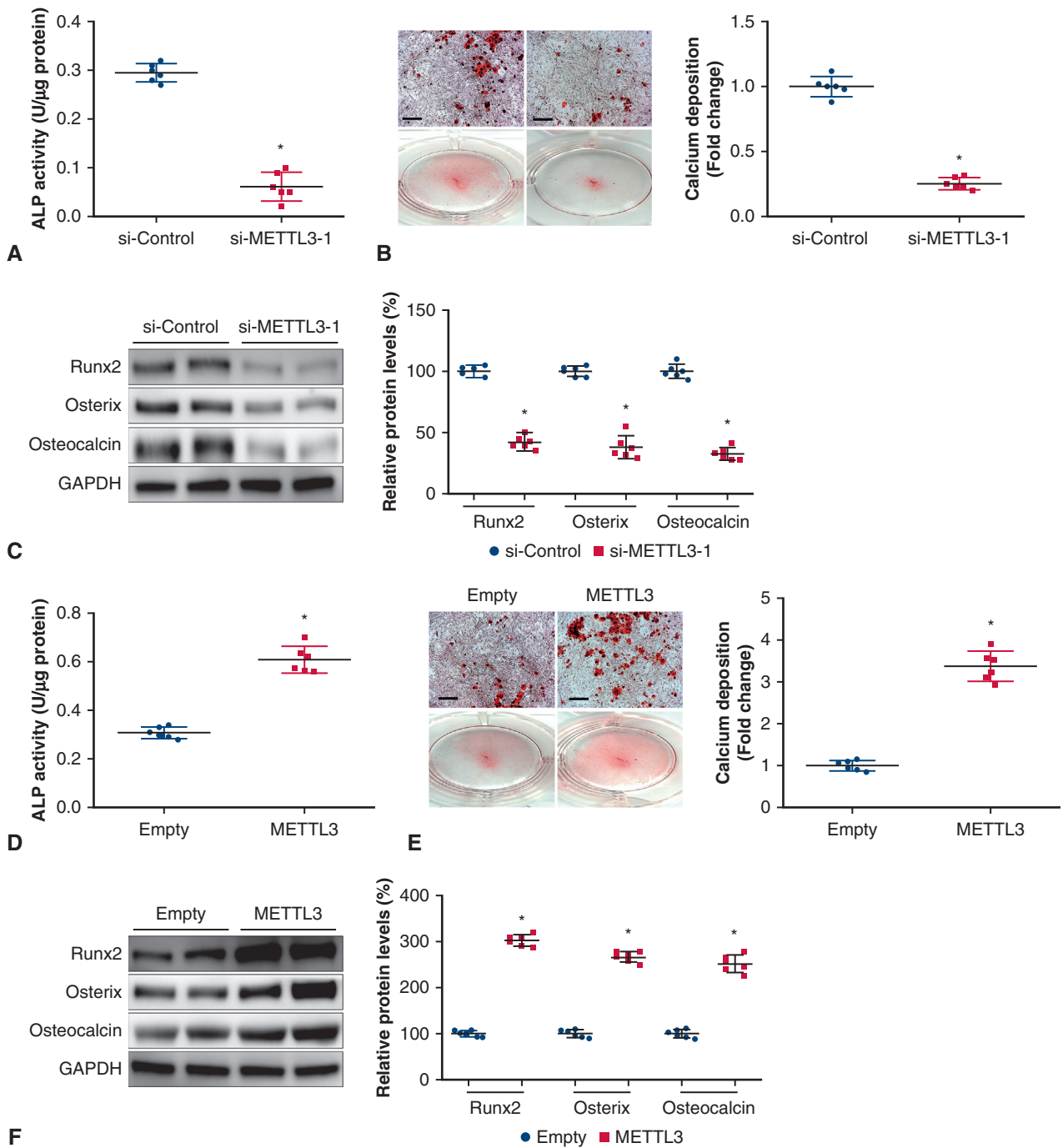
FIGURE E5. METTL3 promotes osteogenic differentiation of hVICs isolated from human calcific aortic valves. METTL3 knockdown in hVICs significantly attenuated the osteogenic medium-induced increase in ALP activities (A), calcified nodule formation (B), and protein levels of 3 osteogenesis-specific markers (Runx2, Osterix, and Osteocalcin) (C). METTL3 overexpression in hVICs promoted the osteogenic medium-induced increase in ALP activities (D), calcified nodule formation (E), and protein levels of osteogenesis-specific markers (F). Scale bar: 50 μm. *P < .05 versus control or empty. *si-Control*, Small interfering RNA for control; *si-METTL3-1*, small interfering RNA for methyltransferase-like 3; *Empty*, Empty vector; *GAPDH*, glyceraldehyde-3-phosphate dehydrogenase.
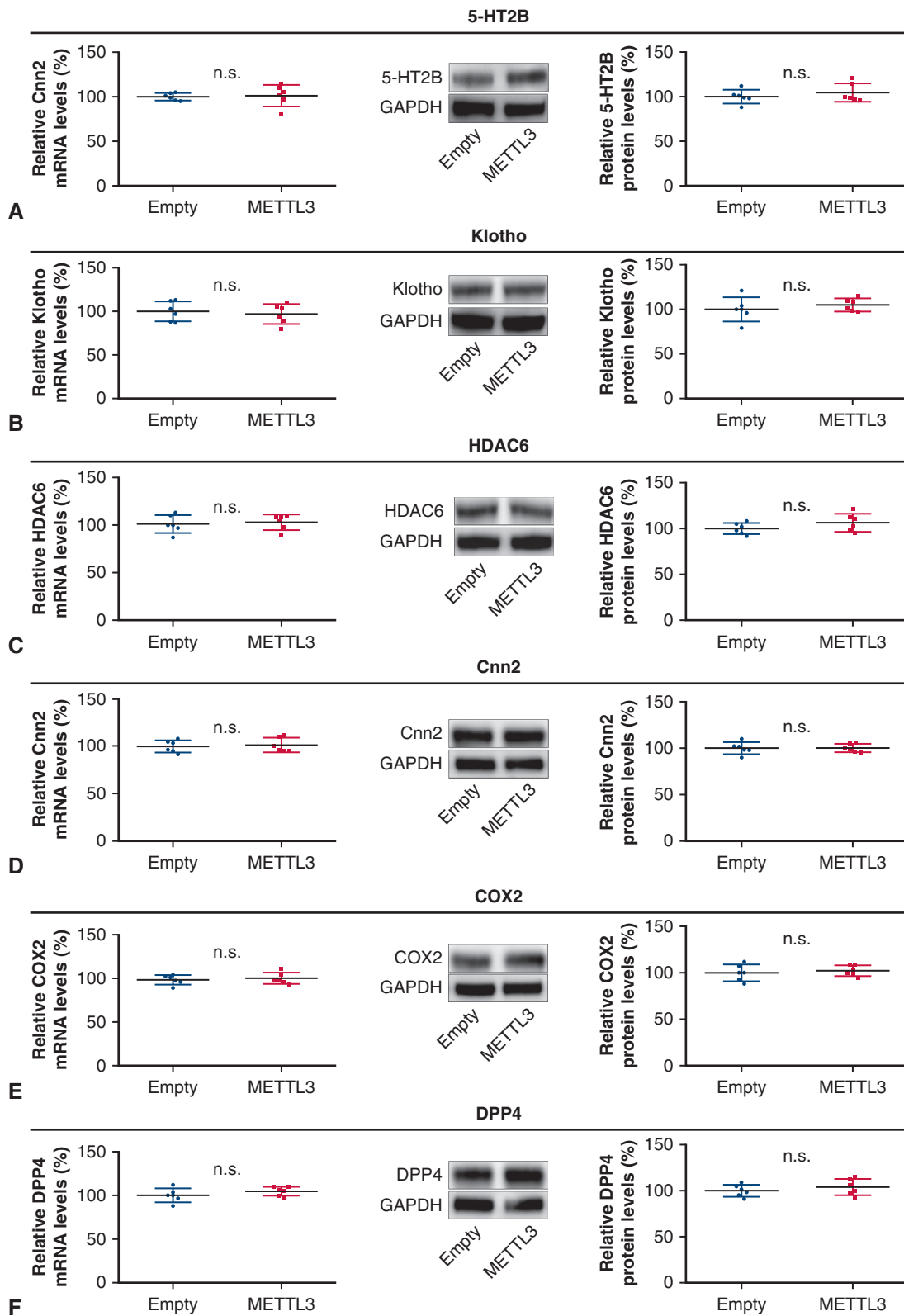
FIGURE E6. METTL3 overexpression had no effect on the mRNA and protein levels of serotonin 2B receptor (A), Klotho (B), histone deacetylase 6 (C), calponin 2 (D), cyclooxygenase 2 (E), and dipeptidyl peptidase-4 (F). *Empty*, Empty vector; *n.s.*, not significant; *GAPDH*, glyceraldehyde-3-phosphate dehydrogenase.
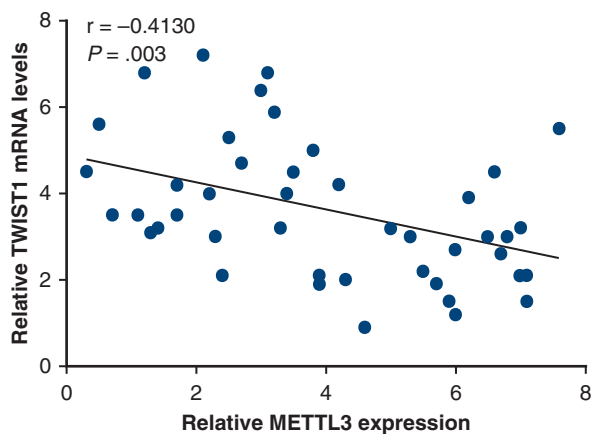
FIGURE E7. Correlation analysis between TWIST1 and METTL3 among human CAVS (n = 50) as indicated by 2-tailed Pearson's correlation analysis.
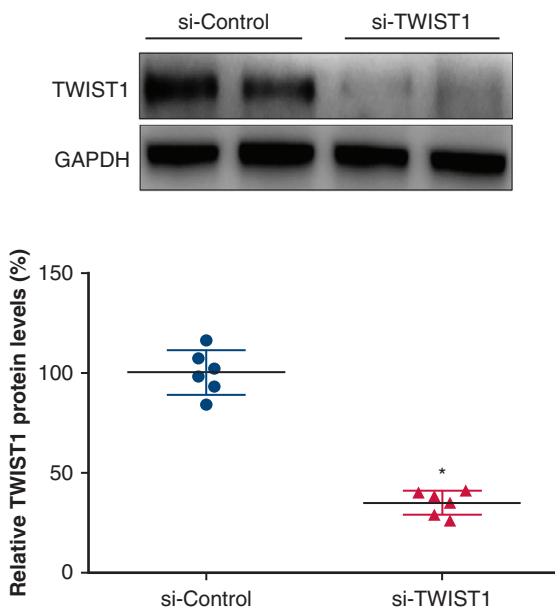
FIGURE E8. TWIST1 silencing in hVICs was confirmed by Western blot. *P < .05 versus si-Control. *si-Control*, Small interfering RNA for control; *si-TWIST1*, small interfering RNA for twist-related protein 1.

TABLE E1. Clinical characteristics of patients for cell cultures

Parameters	Control valves (n = 10)
Age, y	55 ± 2
Male (%)	66
BMI (kg/m^2)	22.9 ± 2.7
Hypertension (%)	51
Triglycerides (mmol/L)	1.55 ± 0.31
LDL (mmol/L)	2.21 ± 0.26
HDL (mmol/L)	1.36 ± 0.30
Diabetes mellitus (%)	33
Smoking (%)	75
Statins (%)	75
β-blockers	70
ACEi/ARB	68
LVEF (%)	59.8 ± 5.20
Bicuspid aortic valves (%)	0
Transvalvular gradient (mm Hg)	16.80 ± 3.55
AVA (cm^2)	3.20 ± 0.30

Values are mean ± standard deviation or %. *BMI*, Body mass index; *LDL*, low-density lipoprotein cholesterol; *HDL*, high-density lipoprotein cholesterol; *ACEi*, angiotensin-converting enzyme inhibitor; *ARB*, angiotensin receptor blocker; *LVEF*, left ventricular ejection fraction; *AVA*, aortic valve area.

TABLE E2. Small interfering RNA sequences

siRNA	Sequence (5′ to 3′)
METTL3-siRNA-#1	CTGCAAGTATGTTCACTATGA
METTL3-siRNA-#2	GCUACCGUAUGGGACAUUA
TWIST1-siRNA	AAGCTGAGCAAGATTCAGACC
YTHDF2-siRNA	GCCCAAUAAUGCAUAUACUTT

siRNA, Small interfering RNA.

TABLE E3. Clinical characteristics of patients for quantitative reverse transcription-polymerase chain reaction analysis

Parameters	Control (n = 50)	CAVS (n = 50)	P value
Age, y	56 ± 2	57 ± 4	.117
Male (%)	64	68	.407
BMI (kg/m^2)	20.25 ± 1.98	21.01 ± 2.56	.100
Hypertension (%)	50	48	.780
Triglycerides (mmol/L)	1.42 ± 0.11	1.49 ± 0.26	.083
LDL (mmol/L)	1.79 ± 0.22	1.85 ± 0.30	.257
HDL (mmol/L)	1.39 ± 0.18	1.40 ± 0.28	.832
Diabetes mellitus (%)	28	26	.657
Smoking (%)	72	68	.390
Statins (%)	62	56	.251
β-blockers	66	60	.229
ACEi/ARB	70	66	.399
LVEF (%)	60.50 ± 3.25	59.50 ± 2.10	.070
Transvalvular gradient (mm Hg)	16.60 ± 2.15	89.50 ± 6.58	<.0001
AVA (cm^2)	2.95 ± 0.28	0.69 ± 0.09	<.0001

Values are mean ± standard deviation or %. *CAVS*, Calcific aortic valve stenosis; *BMI*, body mass index; *LDL*, low-density lipoprotein cholesterol; *HDL*, high-density lipoprotein cholesterol; *ACEi*, angiotensin-converting enzyme inhibitor; *ARB*, angiotensin receptor blocker; *LVEF*, left ventricular ejection fraction; *AVA*, aortic valve area.

TABLE E4. Primers for quantitative real-time polymerase chain reaction

Genes	Primer sequence (5′ to 3′)
METTL3 forward	ATCCCCAAGGCTTCAACCAG
METTL3 reverse	GCGAGTGCCAGGAGATAGTC
TWIST1 forward	GTCCGCAGTCTTACGAGGAG
TWIST1 reverse	TCCATCCTCCAGACCGAGAAG
METTL14 forward	AGAGAACAAAGGAACACTGCCT
METTL14 reverse	AATGAAGTCCCCGTCTGTGC
WTAP forward	ACGCAGGGAGAACATTCTTG
WTAP reverse	CACACTCGGCTGCTGAACT
YTHDF1 forward	ATGTCGGCCACCAGCGTGGACA
YTHDF1 reverse	TCATTGTTTGTTTCGACTCTGC
YTHDF2 forward	TAGCCAACTGCGACACATTC
YTHDF2 reverse	CACGACCTTGACCTTCCTTT
RUNX2 forward	AGCTTCTGTCTGTGCCTTCTGG
RUNX2 reverse	GGAGTAGAGAGGCAAGAGTTT
Osterix forward	GACTGCAGAGCAGGTTCCTC
Osterix reverse	TAACCTGATGGGGTCATGGT
Osteocalcin forward	CTCTCTCTGCTCACTCTGCT
Osteocalcin reverse	TTTGTAGGCGGTCTTCAAGC
GAPDH forward	AACGTGTCAGTGGTGGACCTG
GAPDH reverse	AGTGGGTGTCGCTGTTGAAGT
Cnn2 forward	GAGACCTGGGCTTGGAAG
Cnn2 reverse	CTGAAACTTGCGGGCATA
Cox2 forward	AGTATCACAGGCTTCCATTGACCAG
Cox2 reverse	CCACAGCATCGATGTCACCATAG
DPP4 forward	GCACGGCAACACATTGAA
DPP4 reverse	TGAGGTTCTGAAGGCCTAAATC